



Simulative investigation of wind turbine gearbox loads during power converter fault

Julian Röder¹ · Georg Jacobs¹ · Tobias Duda¹ · Dennis Bosse¹ · Fabian Herzog¹

Received: 16 November 2020 / Accepted: 4 March 2021 / Published online: 26 March 2021
© The Author(s) 2021

Abstract

Three phase short circuit power converter faults in wind turbines (WT) result in highly dynamic generator torque reversals, which lead to load reversals within the drivetrain. Dynamic load reversals in combination with changing rotational speeds are, for example, critical for smearing within roller bearings. Therefore, an investigation of the correlation between three phase short circuit converter faults and drivetrain component failures is necessary.

Due to the risk of damage and the resulting costs, it is not economically feasible to extensively investigate three phase short circuit converter faults on test benches. Valid WT drivetrain models can be used instead. A WT drivetrain model, which has been developed and validated in a national project at the CWD, is used and a three phase short circuit converter fault is implemented. In this paper, the resulting torque load on the drivetrain for a three phase short circuit converter fault in rated power production is presented. This converter fault leads to a highly dynamic reversing electromagnetic torque which exceeds the rated torque by a factor of three. As a result the load on the rotor side high speed shaft (HSS) bearing oscillates and increases by around 15 per cent compared to rated power production. Simultaneously the rotational velocity of the HSS oscillates with an amplitude of 10rpm. Therefore an increase in the risk of smearing is expected.

Simulative Untersuchung der Getriebelasten einer Windenergieanlage während eines Umrichterfehlers

Zusammenfassung

Dreiphasige Kurzschlüsse in den Umrichtern von Windenergieanlagen (WEA) führen zu hochdynamischen Drehmomentanregungen des Generators. Die hochdynamischen Generatoranregungen führen zu hochdynamischen Anregungen des mechanischen Triebstrangs und damit zu Lastwechseln in den Komponenten. Dynamische Lastwechsel in Kombination mit wechselnden Drehzahlen sind kritisch für dynamisch getriebene Schäden (z.B. Anschmierungen in WEA-Getriebewälzlagern). Deshalb ist eine Untersuchung des Zusammenhangs zwischen dreiphasigen Umrichter Kurzschlüssen und Schäden an mechanischen WEA-Triebstrang-Komponenten notwendig. Aufgrund des Risikos für Schäden an der WEA und des Prüfstandes ist es wirtschaftlich nicht sinnvoll, Umrichter Kurzschlüsse auf Prüfständen zu untersuchen. Stattdessen können validierte Simulationsmodelle genutzt werden. In dieser Studie wird das validierte Simulationsmodell der Forschungswindenergieanlage (FVA-Gondel) des CWD verwendet, ein dreiphasiger Kurzschluss zwischen Generator und Umrichter implementiert und dessen Auswirkung auf den mechanischen Triebstrang untersucht. Der Umrichter Kurzschluss führt zu einer hochdynamischen Anregung des Generatormoments mit signifikanter Momentenüberhöhung. Als Folge der Anregung oszilliert die Radiallast des rotorseitigen Zylinderrollenlagers an der schnell drehenden Welle (HSS) des Triebstrangs und überhöht initial um 15 Prozent. Gleichzeitig oszilliert die HSS-Drehzahl. Folglich ist eine Erhöhung des Risikos für Anschmierungen zu erwarten.

✉ Julian Röder
julian.roeder@cwd.rwth-aachen.de

¹ Center for Wind Power Drives, RWTH Aachen University,
52074 Aachen, Germany

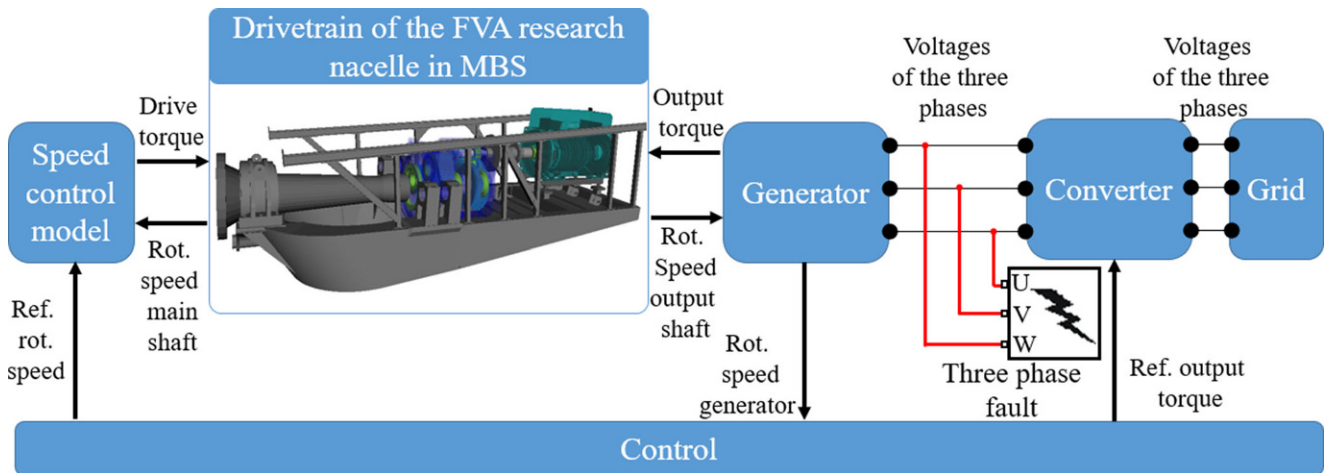


Fig. 1 Schematic of the WT model with the three phase fault

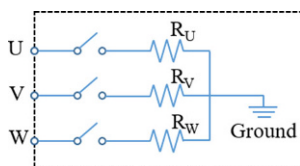


Fig. 2 Schematic of the three phase fault between generator and converter

1 Motivation

The importance of wind energy in the energy supply of the future will increase in coming years while costs for WTs steadily fall [1]. One driver for WT costs is the reliability. In order to improve the reliability all loads during the lifetime need to be considered in the design process. The loads on drivetrain components resulting from the wind are dependent on various aspects, e.g. the rotor blade design. The drivetrain is also loaded by the generator, the power converter and the grid. During normal operation of the WT the load resulting from the generator, the power converter and the grid is quasi static.

Highly dynamic generator torque excitations can, for example, occur as a result of a three phase short circuit due to a damage in the machine-side phase module of the power converter resulting in a permanent conducting state. According to Scott [2] and Bartschat [3] WT power converters have a high failure rate. These failures include minor faults e.g. in the software that can be cleared fast as well as major faults e.g. in the phase modules [3]. In a preliminary study at the CWD a converter fault has been emulated via a crowbar set up for an idling WT drivetrain. The resulting generator torque lead to a highly dynamic HSS excitation with torque ramps of up to of 418 kNm/s [4]. Furthermore, Heier [5] states that converter damages resulting in a three phase fault between the generator and the converter during power production can lead to highly dynamic torque excitations that exceed the rated torque by factors of up to

six. These dynamic excitations can have a negative impact on the lifetime of the components within the drivetrain. Highly dynamic load reversals in combination with significant slip induced by changing rotational speeds are, for example, critical for smearing within roller bearings, e.g. in WT gearboxes [6, 7]. Faults in the gearbox are the main driver for WT downtimes [2]. This is due to the length of time to repair the gearbox fault. Within the gearbox the HSS bearings account for around 40 per cent of failures [2, 8]. Therefore, it is necessary to investigate the correlation between three phase short circuit converter faults and HSS bearing damages. It is not economically feasible to do the investigation via extensive tests on a WT test bench because of the high risk of damages to the WT components and the test bench. Instead, valid WT drivetrain models can be used.

2 Approach

A model of a WT is used in order to investigate the influence of a three phase short circuit converter fault on the loading of drivetrain components. The model specifics are discussed in Chap. 3. In Fig. 1 the schematic framework of the WT model is shown. A three phase fault is implemented between the generator and the converter in order to emulate the three phase short circuit converter fault. The three phase fault has the same effect as a damage in the machine-side phase module of the converter resulting in a permanent conducting state.

The model of the three phase fault is set up as a three phase circuit breaker (see Fig. 2). All three fault resistances R_U , R_V and R_W are set to a low value of 0.001Ω . The closing time of the breaker is set to $t = 10s$ for all three phases U, V and W which results in a state similar to a short circuit between the three phases and the ground.

Fig. 3 Stator currents (a) and highly dynamic electromagnetic generator torque reversal (b) after the three phase short circuit converter fault

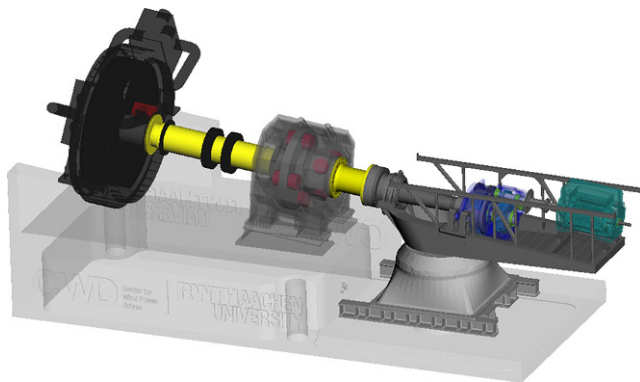
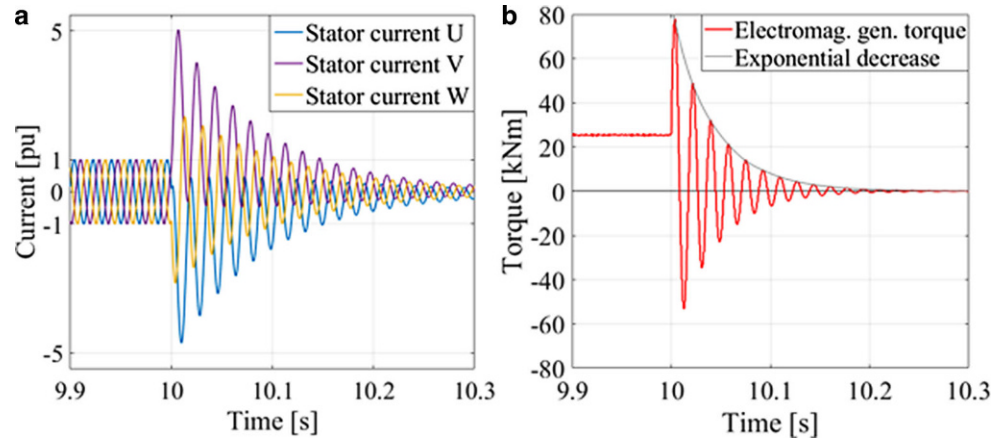


Fig. 4 MBS model of the research nacelle on the test bench at the CWD

In Fig. 3 (left) the stator currents and the electromagnetic generator torque (right) for a converter fault at $t = 10$ s during rated power production are shown. Due to the short circuit the stator voltage drops and the stator current surges. Accordingly, the generator torque increases rapidly [5, 9, 10]. The highest peak in the electromagnetic generator torque exceeds the rated torque by a factor of around three. This significant overload could be detrimental to the coupling between generator and gearbox as well as to the components within the gearbox [5]. After the initial peak the generator currents start to decline exponentially since the stator voltage approaches zero. The time constant τ_s of

the exponential decrease can be calculated with the following equation [10]:

$$\tau_s = \frac{L_s + \frac{R_r + X_r}{R_r + X_r + X_m} \cdot L_m}{R_s} \tag{1}$$

Here L_s and R_s are the stator leakage inductance and resistance, L_r and R_r are the rotor leakage inductance and resistance and L_m is the magnetizing inductance of the generator. X_r and X_m are the rotor and magnetizing reactances, respectively. This yields a time constant of $\tau_s = 109.5$ ms for the given generator and operating point. The electromagnetic torque declines exponentially as well and reaches nearly zero after 0.3 s. The electromagnetic torque excitation is calculated in Simulink and connected to the MBS model of the drivetrain via co-simulation. The resulting drivetrain loads are discussed in Chap. 4.

3 Models

The model of the WT (see Fig. 1) connects the MBS model of the research nacelle drivetrain with analytical models for the control, the generator, the power electronics and the grid via co-simulation in Matlab Simulink [11, 12]. The MBS model also includes the test bench (see Fig. 4). The test bench model is used because it has been validated via extensive tests according to IEC 61400 [11, 12]. Additionally, tests regarding a converter fault emulated via a crowbar set up with the WT research nacelle in idling mode, i.e. without power production, were conducted. The tests with the crowbar set up lead to a highly dynamic torque excitation. Using the measurement data it was possible to validate the dynamic behaviour of the MBS drivetrain model during this fault [4, 13].

The control model emulates the behaviour of the nacelle during power production. The load on the HSS due to the converter fault is the focus of this paper. Therefore, the

Table 1 Specification of the generator of the research nacelle

Specification	Value
Type	Asynchronous
Number of pole pairs	3
Apparent power	3 MVA
Rated voltage	720 V
Rated current	2564 A
Rated torque	24.7 kNm
Rated rotational velocity HSS	1100 rpm

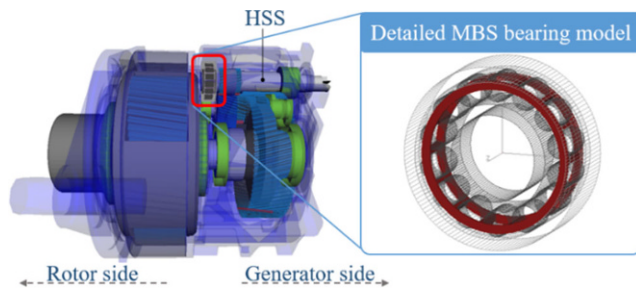


Fig. 5 MBS gearbox model of the research nacelle (left) with the detailed bearing model (right)

loading due to the wind is simplified by a speed control model disregarding the non-torque loads. The speed control sets a torque with regard to the actual speed and the reference. The torque is applied to the drivetrain via the motor model (see Fig. 4). Accordingly, the HSS rotates with a rated rotational speed of around 1100rpm until the fault is triggered.

The model of the electric system consists of a generator model, a model of the full size power converter and a model of the grid. The generator is modelled as a three phase asynchronous induction machine. The parameters of the generator are implemented according to manufacturer's data (see Table 1). The analytic generator model represents the fundamental waves of the electromagnetic force generation. This modelling depth was determined to be sufficient for the investigation of damage relevant loads within the drivetrain of the turbine [11].

The full size converter model was modelled according to state of the art guidelines. The grid model is a parameter model only representing its inductances [11]. In order to emulate a three phase short circuit converter fault, a three phase short circuit is implemented between the converter and the generator (see Figs. 1 and 2).

FE-models have been set up and modally reduced in order to implement the stiffness characteristics and deformations of all relevant components in the MBS model. By taking into account all relevant deformations of the research nacelle and the test bench it is possible to calculate internal load states [11, 12]. The gearbox has one planetary stage followed by two helical gear stages with a resulting gear ratio of 62.775. The gear pairs are modelled using a gear pair force element including backlash. The bearing characteristics are implemented based on manufacturer data via force elements using one dimensional curves for radial and axial direction including non-linearity and clearance [12].

For the investigation of the bearing loads at individual rollers a detailed MBS model (see Fig. 5, right) developed by the drivetrain research association (FVA) [14] is implemented on the rotor side of the HSS. This model explicitly represents the outer ring, inner ring, cage and rollers as well as the lubricant.

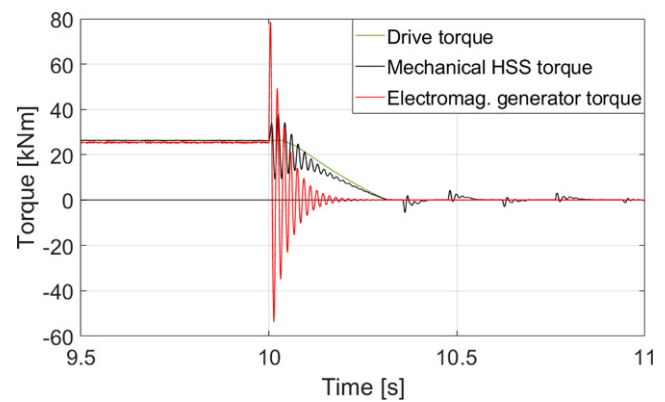


Fig. 6 Electromagnetic, HSS, and drive torque normalized by the gearbox ratio

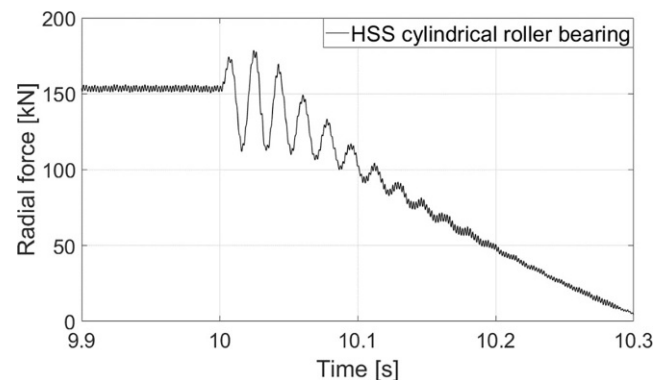


Fig. 7 Radial load of the cylindrical roller bearing

4 Results

The torque load for the three phase short circuit converter fault during rated power production for the generator, the HSS and the drive is shown in Fig. 6. The electromagnetic torque reverses with a frequency of 54.5Hz which corresponds to the nominal frequency of the stator currents. The generator is coupled to the HSS via a steel disk coupling which is modeled using design parameters supplied by the manufacturer [11]. Therefore, peaks in the generator torque are damped. The drive still applies the rated torque (see Fig. 6, green line) for around two cycle times until the controller decreases the drive torque. The drive torque reaches zero, 0.3s after the fault occurs. The drive torque decreases slower than the generator torque due to the high inertia. As a result the HSS torque (see Fig. 6, black line) is not as dynamic as the generator torque. 0.3s after the fault occurs, neither the drive nor the generator excite the drivetrain. Therefore after $t = 10.3$ s the HSS torque oscillates with the first natural torsional frequency of the drivetrain on the test bench of around 6Hz (see Fig. 6).

The torque excitation (see Fig. 6) leads to an oscillating radial force (see Fig. 7) on the inner ring of the rotor side HSS bearing (see Fig. 5). The radial force increases initially

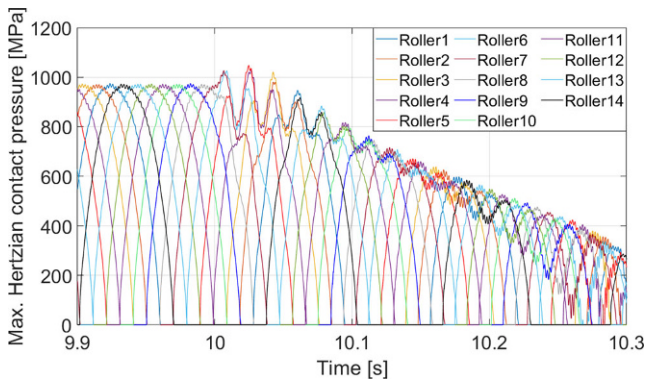


Fig. 8 Maximum Hertzian contact pressure for each roller and the inner ring

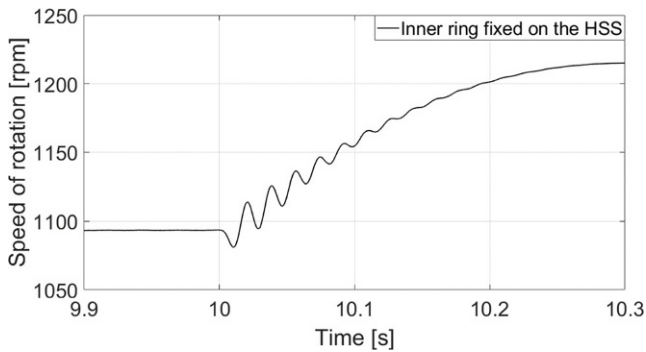


Fig. 9 Speed of rotation of the inner ring of the bearing model

by around 15 per cent of the rated force. After 0.3 s of the initial increase the radial load of the bearing diminishes almost completely due to the decreasing applied torques (see Fig. 6).

The radial bearing load on the inner ring (see Fig. 7) is distributed to several rollers in the load zone [15]. During the converter fault starting at $t = 10$ s the contact force between the inner ring and the rollers in contact increases. Accordingly, the maximum Hertzian contact pressure [16] between the rollers and the raceway increases by a maximum of around 5 per cent before it decreases (see Fig. 8).

The inner ring of the bearing is fixed on the HSS. In Fig. 9 the speed of rotation of the inner ring of the bearing model during the fault is shown. Initially after the converter fault at $t = 10$ s the electromagnetic generator torque exceeds the drive torque (see Fig. 6). Therefore, the rotational speed decreases initially. Due to the reversing generator torque with peaks in both negative and positive direction the rotational speed of the HSS oscillates with an amplitude of 10 rpm. The controller decreases the drive torque to zero, 0.3 s after the fault occurs. Due to the high inertia of the rotor the driving torque decreases slower than the generator torque. Therefore, the rotational speed of the HSS increases to a maximum of around 1220 rpm before it idles until stillstand.

Due to the oscillating rotational speed in combination with the load reversal it is possible that there is a severe increase in slip between the rollers and the raceways. As a result of the oscillating load in combination with the increase of slip it is likely, that the risk of smearing during the short circuit converter fault increases for the rotor side HSS bearing [6, 7, 17].

5 Outlook

The kinematics of each roller in combination with the loading will be used for the evaluation of the risk of smearing by calculation of a smearing criterion. There are different state of the art smearing criterions [6, 7, 17–19] that are all based on energetic equations. Fundamental to these equations is the friction power intensity [17]. Dyson [17] concluded that the occurrence of smearing during tribotesting is always accompanied by an increase in measured friction. Dyson also stated that smearing can only be generated when significant slip is present between the contact partners. In analogy to the state of the art van Lier [6] defined a smearing criterion which is based on the power P per loaded area A :

$$\left(\frac{P}{A}\right)_{\max} = \max(0.5 \cdot \mu(t) \cdot p_{\max}(t) \cdot (u_1(t) - u_2(t))) \quad (2)$$

$\mu(t)$ describes the friction coefficient for the contact between the roller and the raceway, p_{\max} is the maximum Hertzian contact pressure and $u_1(t) - u_2(t)$ describes the sliding speed between the roller and the raceway. In order to estimate the risk of smearing the value of the criterion can be compared to state of the art thresholds which range from $1.05 \cdot 10^8$ to $1.4 \cdot 10^8$ [19], to $1.5 \cdot 10^8$ [18] to $2.6 \cdot 10^8 \text{ W} \cdot \text{m}^{-2}$ [7]. By comparing the simulation results to these thresholds, it is possible to evaluate the smearing risk within WT bearings for three phase short circuit converter faults. The analysis of the roller kinematics and the smearing criterion will be part of future works.

Furthermore, local loads on the gear flank and in the tooth root of the gear during short circuit converter faults will be investigated. This will be done in cooperation with the Laboratory for Machine Tools and Production Engineering (WZL) by using detailed FE based tooth contact models [20].

The models will also be used to conduct extensive simulative investigations regarding the drivetrain loads during grid faults with the WT research nacelle in doubly fed induction generator (DFIG) configuration.

6 Conclusion

A simulative approach for the investigation of WT drive-train loads during a three phase short circuit converter fault has been presented in this paper. The results of the HSS bearing loads were shown exemplarily. The short circuit converter fault was simulated via a three phase short circuit between the generator and the converter. This configuration has the same effect as a damage in the machine-side phase module of the power converter resulting in a permanent conducting state. It was shown that the fault results in a highly dynamic reversing electromagnetic torque excitation. During the fault the HSS torque in the WT model is oscillating but not reversing. This is due to the steel disk coupling between HSS and generator, the inertia of the rotor and the driving torque. By analysis of the internal bearing loads during the fault it was shown that the radial load of the bearing is oscillating during the fault and increases by a maximum of 15 per cent compared to the load in rated power production. Simultaneously the rotational velocity of the HSS oscillates with an amplitude of 10rpm. Therefore an increase in the risk of smearing is expected. There is also the possibility to calculate the kinematics of the HSS bearings rollers with the detailed MBS model. The analysis of the roller kinematics and the final analysis of the smearing criterion for the HSS bearing during the three phase short circuit converter fault will be part of future works.

Acknowledgements The authors would like to thank the Ministry of Economic Affairs, Innovation, Digitalization and Energy of the State of North Rhine-Westphalia, Germany, for the financial support granted. They also thank their project partners for the equipment, insight as well as expertise they have provided, which contributed to this joint project.



EUROPÄISCHE UNION
Investition in unsere Zukunft
Europäischer Fonds
für regionale Entwicklung



EFRE.NRW
Investitionen in Wachstum
und Beschäftigung

Funding Open Access funding enabled and organized by Projekt DEAL.

Open Access This article is licensed under a Creative Commons Attribution 4.0 International License, which permits use, sharing, adaptation, distribution and reproduction in any medium or format, as long as you give appropriate credit to the original author(s) and the source, provide a link to the Creative Commons licence, and indicate if changes were made. The images or other third party material in this article are included in the article's Creative Commons licence, unless indicated otherwise in a credit line to the material. If material is not included in the article's Creative Commons licence and your intended use is not permitted by statutory regulation or exceeds the permitted use, you will need to obtain permission directly from the copyright holder. To view

a copy of this licence, visit <http://creativecommons.org/licenses/by/4.0/>.

References

- Rohrig K (2019) Powering the 21st century by wind energy—Options, facts, figures. *Appl Phys Rev* 6(3). <https://doi.org/10.1063/1.5089877>
- Scott K (2012) Effects of extreme and transient loads on wind turbine drive trains. In: AIAA meeting paper of 50th AIAA aerospace sciences meeting Nashville
- Bartschat A (2018) Zuverlässige Leistungselektronik für Windenergieanlagen. IWES final report. Fraunhofer Verlag,
- Duda T (2018) Investigation of dynamic drivetrain behaviour of a wind turbine during a power converter fault. *J Phys* 1037(5):1456–1463
- Heier S (2018) Windkraftanlagen – Systemauslegung, Netzintegration und Regelung, 6th edn. Springer Vieweg, Wiesbaden
- Van Lier H (2015) Schädlicher Wälzlagerschlupf. FVA final report 1124
- Evans R (2013) Prevention of smearing damage in cylindrical roller bearings. *Tribol Trans* 56:703–716
- Guo Y (2018) Rolling element bearing dynamics in wind turbines. NREL Engineering Technical Conferences Meeting, NREL/PR-5000-72185, American Society of Mechanical Engineers International Design.
- Fischer R (2017) Elektrische Maschinen, 17th edn. Hanser, München
- Bin Wu (2011) Power conversion and control of wind energy systems. John Wiley & Sons, New Jersey
- Matzke D (2017) Full scale system simulation of a 2.7 MW wind turbine on a system test bench. In: Proc. of conf. for wind power drives Aachen, pp 241–254
- Matzke D (2019) Validation of MBS modelling methods to calculate bearing and tooth loads in the planetary gear stage of a wind turbine. In: Proc. of conf. for wind power drives Aachen, pp 333–347
- Röder J (2020) Simulative investigation of the load propagation in a wind turbine drive train during a power converter fault. *J Phys* 1618(3). <https://doi.org/10.1088/1742-6596/1618/3/032028>
- Kiebusch T (2017) Zylinderrollenlagermodul für Simpack – Entwicklung eines Berechnungsmoduls zur Dynamiksimulation und Betriebsanalyse von Zylinderrollenlagern unter Berücksichtigung der Umgebungskonstruktion in Simpack. FVA Forschungsvorhaben Nr. 625 II. final report 1124
- Nguyen-Schäfer H (2016) Computational design of rolling bearings, 1st edn. Springer, Berlin
- Hertz H (1881) Über die Berührung fester elastischer Körper. *J Reine Angew Math* 92:156–171
- Dyson A (1975) Scuffing—a review. *Tribol Int* 8:77–87
- Bujoreanu C (2003) Scuffing behaviour in angular contact ball bearings. Annals of Dunarea de Jos University of Galati., Tribology
- Fowel M (2014) An Experimental Investigation into the Onset of Smearing Damage in Nonconformal Contacts with Application to Roller Bearings. *Tribol Trans* 57:472–488
- Theling J (2019) Influence of planet carrier misalignments on the operational behaviour of planetary gearboxes. In: Proc. of 8th WZL Gear Conference, chapter 14 Denver. In, Colorado